Phthalocyanine-based Hybrid Catalyst for Rechargeable Lithium-Oxygen Batteries

Padmakar Kichambare[1], Stanley Rodrigues[2], David Firsich[3], William A. Feld[3],

Perla B. Balbuena[4] and Lawrence Scanlon[2]

[1]UES Inc., 4401 Dayton-Xenia Road, Dayton, OH 45432

[2]Air Force Research Laboratory, Aerospace Systems Directorate

Wright-Patterson Air Force Base, OH 45433

[3] Department of Chemistry, Wright State University, Dayton, OH 45433

[4] Department of Chemical Engineering, Texas A & M University, College Station, TX 77843

Padmakar.Kichambare.1.ctr@US.AF.MIL

Abstract: *A mixture of tetrabutylammonium lithium phthalocyanine (TBA-LiPc) and dilithium phthalocyanine (Li$_2$Pc)) functions as a soluble bifunctional catalyst in tetraethylene glycol dimethyl ether (TEGDME) for a rechargeable lithium-oxygen cell. Cyclic voltammetry (CV) measurements of the hybrid catalyst in TEGDME show highly symmetrical and reversible peaks at 2.54 V and 3.22 V vs Li/Li$^+$, corresponding to the reduction of the peroxide and oxidation of Li$_2$O$_2$, respectively. Density functional theory (DFT) calculation shows that the oxygen complex with the LiPc anion is already in the superoxide state since the oxygen-oxygen bond length is 1.32 Å. Once reduction takes place it goes into the peroxide state, forming lithium peroxide. A Cell with graphene nanosheets (GNSs) coated onto a hierarchical porous carbons (HPC) cathode was discharged to 2V in an oxygen atmosphere, delivering an initial capacity of 20448 mAh/g$_{(carbon)}$. Long-term cycling of cells with GNSs coated HPC cathodes at a fixed capacity of 1200 mAh/g $_{(carbon)}$ in oxygen and dry air (relative humidity < 0.01% at room temperature) is in progress. Cells have completed 295 and 284 cycles in oxygen and dry-air, respectively.*

Keywords: lithium-air battery; oxygen reduction; oxygen evolution; tetraethylene glycol dimethyl ether; tetra-butyl ammonium lithium phthalocyanine.

Introduction

A lithium-oxygen battery is attractive due to its very large theoretical energy density [1]. The cell operates on a simple chemical reaction between lithium ions and oxygen radicals. Significant efforts have been made to use stable electrolytes and solid-state catalysts decorated on oxygen electrodes to improve the cycling stability and electrocatalytic activity for the oxygen reduction reaction (ORR) and oxygen evolution reaction (OER) [2]. Among various non-aqueous solvents, TEGDME is a promising electrolyte and among catalysts, phthalocyanine based derivatives are also attracting interest as non-precious catalysts. High discharge capacity was reported when Li$_2$Pc was employed as cathode catalyst [3]. In other work [4], a solution-phase bifunctional iron phthalocyanine (FePc) catalyst dissolved in TEGDME and dimethyl sulfoxide (DMSO) electrolyte was employed. The FePc catalyst acts as a molecular shuttle of (O$_2$)$^-$ between the surface of carbon cathode and insulator Li$_2$O$_2$, product of discharge. Recently transition metal phthalocyanines were used as solution phase redox mediators in rechargeable lithium-oxygen batteries [5]. It is reported that redox mediation for the Mn, Co, and Ni configuration is better than Fe and Cu configuration.

In continuation of our work [6], we report here the use of GNSs coated HPC as an oxygen cathode with a mixture of two moles of TBA-LiPc and one mole of a Li$_2$Pc as soluble hybrid catalyst in TEGDME electrolyte. TEGDME was selected due to its electrochemical stability over a wide a potential window and good oxygen solubility (4.43 mM/cm^3) [7]. To lower the over-potential, LiI was used as redox mediator. During the charge, LiI is oxidized at the cathode and oxidized form of redox mediator then chemically reacts with Li$_2$O$_2$ and suppress the charge voltage [8].

Experimental Details

Synthesis of HPC was carried using zinc oxide nanoparticles as a hard template. This HPC powder was

used to fabricate the oxygen cathode. Lithium bis(fluorosulfonyl)imide (LiFSI) (Sigma-Aldrich) was dried overnight under vacuum at 120 °C, prior to use. Li_2Pc was purchased (Signa-Aldrich) and purified into acetone by crystallization process. TBA-LiPc catalyst was synthesized and purified. Both catalysts were vacuum dried at 110 °C before use. Electrolyte was prepared by mixing 1.5 M LiFSI, 50 % v/v (0.2 M Li_2Pc and 0.4M TBA-LiPc), 0.4 M LiI, and 3 wt. % FEC (fluoroethylene carbonate) (Sigma-Aldrich) into a mixture of TEGDME (Sigma-Aldrich) and TTE (1,1,2,2 – tetrafluoroethyl- 2,2,3,3-tetrafluoro propyl ether) (Sigma-Aldrich) with a ratio of 8:2 (v/v). CV measurements were performed in a standard three-electrode cell configuration using electrolyte solution of LIFSI and hybrid catalyst in TEGDME at 25 °C with a scan rate of 5 mVSec^{-1}. Graphite rod was used as working electrode. Platinum foil was used as the counter and reference electrode. All potentials were measured with respect to standard Pt electrode and converted to Li|Li$^+$ reference scale. The electrolyte solution was purged with argon to remove any dissolved oxygen. The electrolyte was then saturated with oxygen prior to the CV measurements.

To fabricate the oxygen cathode, HPC powder was mixed and dispersed in N-methyl-2-pyrrolidone (NMP) using sonication for 90 min. This process was carried to load cathode material in the open voids of nickel foam that is used as a current collector. 0.1 wt.% GNSs in NMP was drop casted on HPC deposited nickel foam. Subsequently, specimen was dried overnight at 120 °C, under vacuum. Cells with 1.2 cm^2 active area were fabricated using a Swagelok type cell in a dry room. Nickel foam with GNSs coated HPC was used as working cathode, lithium metal as anode and a glass fiber (Whatman, GF-A) separator soaked with soluble hybrid catalyst (mixture of two moles of TBA-LiPc and one mole of Li_2Pc) in the electrolyte 1.5 M LiFSI, 3 wt.% FEC, 0.4 M LiI in TEGDME-TTE. Cells were discharged and charged with a constant current of 50 µA at 25 °C. Galvanostatic charge-discharge measurements of the specimens were conducted using a computer controlled VersaSTAT 4 (Princeton Applied Research) electrochemical workstation.

Results and Discussion

The morphology of cathode examined under SEM reveals a porous architecture with interconnected pore channels. Nitrogen adsorption–desorption isotherm measurements were carried out at 77 K. The Brunauer-Emmett-Teller (BET) surface area of HPC was found to be 1533 m^2/g with a porosity of 47%. The pore size distribution indicates a wide variation from 2 nm to 137 nm. A remarkable nitrogen uptake above the relative pressure ratio of 0.40 was observed in the BET isotherm and is due to condensation of nitrogen in the HPC matrix. Such high porosity facilitates oxygen transport, diffusion of

electrolyte in the cathode matrix and helps to improve cell capacity. The electro-catalytic ability of hybrid catalyst in oxygen saturated electrolyte was evaluated by CV. Cyclic voltammogram (Fig. 1) shows highly symmetrical and reversible ORR and OER peaks at 2.5 V and 3.22 V, respectively with the current peak amplitude of ~0.125 mA/cm^2 for ORR and OER. The ORR peak corresponds to peroxide formation and OER peak for oxidation of Li_2O_2. The cyclic voltammogram shows no evidence of superoxide oxidation but only lithium peroxide oxidation at 3.2 V. The peak separation of the cathodic (2.5 V) and anodic potential (3.2 V) is found to be 700 mV. The CV study indicates that the oxygen reduction in the presence of hybrid catalyst is reversible. Theoretical calculations have
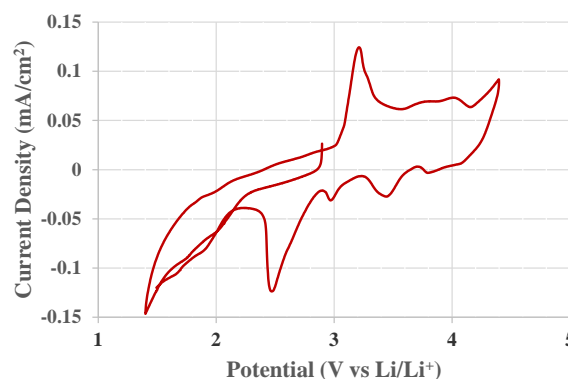

Figure 1. Cyclic voltammogram of (TBA-LiPc-Li_2Pc) as a hybrid catalyst in oxygen saturated electrolyte with a scan rate of 5 mV/sec at room temperature.

shown that the site for oxygen interaction when using TBA-LiPc as the catalyst is located with the lithium-ion in the center of lithium-phthalocyanine anion [6]. With the hybrid catalyst, it is proposed that the Li-Pc anion acts as the main site for oxygen complex formation. The oxygen complex formed in the superoxide state, prior to electrochemical reduction, is due to the electrostatic interaction between oxygen and the lithium-ion resulting in an elongation of the oxygen-oxygen bond (1.32 Å). It is this type of complex that is involved in the reduction of oxygen to peroxides and subsequent re-oxidation to oxygen.

To understand the mechanism of interaction of oxygen with the phthalocyanine, the density functional theory (DFT) was used to investigate the behavior of molecular oxygen near a TBA cation and a LiPc anion. Fig 2 shows the interaction of oxygen in the triplet state with the lithium-ion in the center of the LiPc anion. The resulting complex shows that there is an increase in the oxygen-oxygen bond length to a value of 1.32 Å when compared to a bond length of 1.2 Å for a gas phase oxygen molecule in the triplet state. This bond elongation resembles that of O_2 molecule adsorbing on a Pt$_2$ cluster forming a triplet superoxol state. The 1.32 Å bond length is also consistent

with the superoxo bond length in lithium superoxide (LiO_2). Correspondingly, upon complex formation, there is a transfer of charge. For the triplet state, the charges of the O atoms are -0.39 and -0.32e while the charge on the Li atom is 0.64e. The charge transfer and O_2 reduction is driven by the P_C anion acting as a catalyst. The long cycle
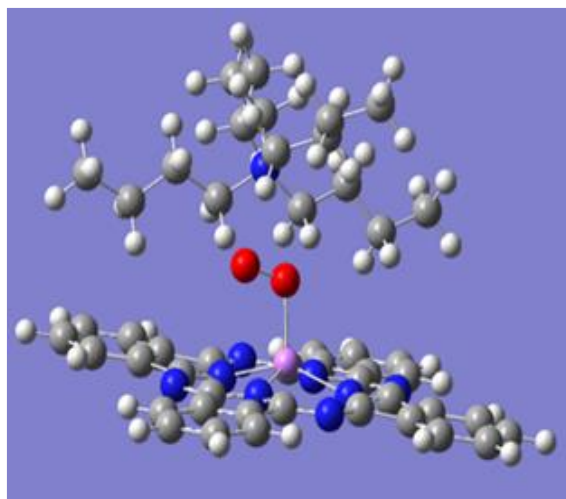

Figure 2. TBA-LiPc interacting with oxygen with spin multiplicity of 3. Geometry was optimized from the MO5-2X functional. Color code: Oxygen atoms are in red, lithium in purple, nitrogen in blue, carbon in grey and hydrogen in white.

times observed in our investigation of the lithium-air battery when using the hybrid catalyst might stem from the fact that the singlet oxygen is complexed and thus unavailable to participate in the electrolyte decomposition process.

Based on the high surface area with the porous structure of HPC and the electro-catalytic activity of the hybrid catalyst towards oxygen reduction and evolution, the electrochemical performance of hybrid catalyst in TEGDME electrolyte was evaluated in the potential range 2 – 4.3 V in oxygen atmosphere. Two lithium-oxygen cells were assembled, one cell with a cathode composed of only HPC and another cell with GNSs coated HPC. The cells with and without GNSs delivered the initial discharge cell capacity of 20450 mAh/g$_{(carbon)}$ and 14760 mAh/g$_{(carbon)}$, respectively at discharge current of 50 µA in oxygen atmosphere (Fig 3). In our previous work [6], the high capacity of 14264 mAh/g$_{(carbon)}$ s also observed upon deep discharge when using 2mM TBA-LiPc as the catalyst. The source of the extra capacity for the cell with GNSs coated HPC cathode (Fig 3) is associated with graphene and is still being investigated. Hu *et al* reported that a graphene-modified LiFePO$_4$ cathode in Li-ion battery exhibited specific capacity of 208 mAh/g, which is beyond the theoretical capacity of 170 mAh/g [9]. The excess capacity

is attributed to the reversible reduction-oxidation reactions between the lithium ions of the electrolyte and the exfoliated graphene flakes. The main feature of electrochemical reduction of oxygen is exhibited as the flat discharge voltage profile from 2.75 to 2.65 V. The cell polarization value (ΔV) between discharge and charge cycles with and without graphene was ~ 1.45 V. ΔV was selected at the mid-point of discharge and charge cell capacity profiles. High capacity of both the cells in Fig 3 is due to the solution phase reaction involving hybrid catalyst, thereby avoiding reaction products build up on the cathode that shuts down the reaction for oxygen reduction and evolution.
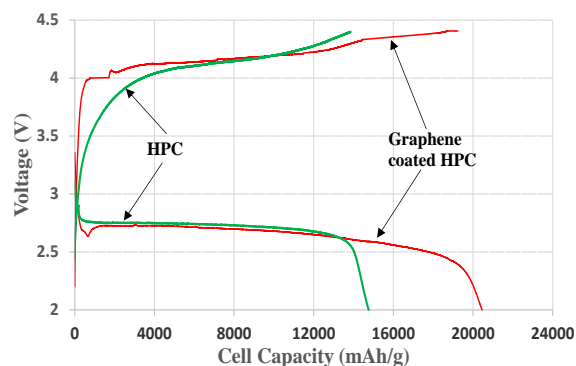

Figure 3. Deep discharge-charge profiles of cells with and without GNSs coated HPC in TEGDME electrolyte in oxygen atmosphere at 25 °C.

Fig 4 shows the long-term cycling stability of a lithium-oxygen cell with GNSs coated HPC cathode in pure oxygen with shallow depth of discharge. Cell was discharged and charged with a constant current of 50 µA for a fixed duration of 11 hours. The cell was operated in the potential range of 2.5 V to 4.2 V.
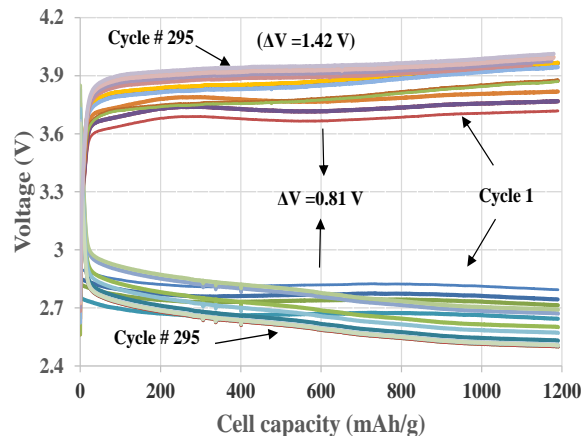

Figure 4. Cycling performance of cell with GNSs coated HPC cathode in TEGDME electrolyte in oxygen atmosphere at 25 °C.

The cell exhibits good cycle performance for 295 cycles with stable reversible capacity of 1190 mAh/g$_{(carbon)}$ in the presence of hybrid catalyst. The cell has an average coulombic efficiency of 97% with ΔV between 1st discharge and 1st charge is 0.81 V. The long cycle life is due to superior electrocatalytic activity of the hybrid catalyst that helps the solution phase formation and oxidation of Li$_2$O$_2$.

Fig 5 shows the cycling behavior of a lithium-air cell with GNSs coated HPC cathode where the source of oxygen is from air inside a dry room. The relative humidity of the air is 0.01 %. The cell was discharged and charged using a constant current of 50 µA for 11 hours (0.55 mAh). The cell was operated in the potential range of 2.4 V (in dry air)
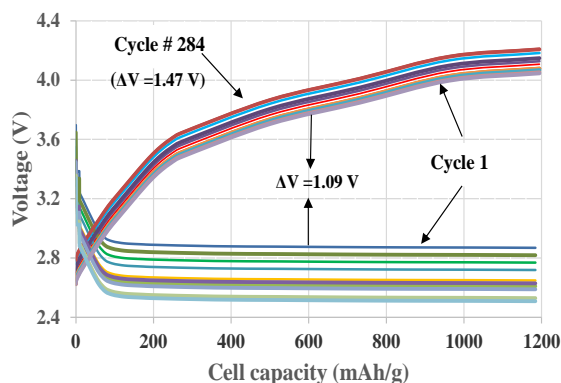

Figure 5. Cycling performance of cell with GNSs coated HPC cathode in TEGDME electrolyte in dry-air atmosphere at 25 °C.

to 4.2 V. The cell exhibits good cycle performance for 284 cycles with stable reversible capacity of 1190 mAh/g$_{(carbon)}$. The cell has an average coulombic efficiency of 97% with ΔV between 1st discharge and 1st charge is 1.01 V. There is a gradual increase in ΔV. At the end of end of 200th cycle, ΔV increased to 1.47 V. The increase in ΔV may be due to the increased thickness of the SEI layer on the lithium metal anode.

Conclusion

In conclusion, CV study demonstrates the significance of a mixture of TBA-LiPc and Li$_2$Pc as bifunctional catalyst in TEGDME. The catalyst plays a key role in promoting a solution phase process for reversible formation and oxidation of the peroxide anion in a low-donor-number solvent. Long-term cycling of lithium-oxygen / lithium-air cells coupled with theoretical calculations strongly suggests the importance of oxygen complexation with the LiPc anion as the first step in reduction of molecular oxygen when using a low-donor-number solvent. It is through this interaction that a long cycle life of over 280

cycles is possible and provides valuable insight of the factors affecting rechargeability of lithium-air cells.

References:

1. Kwak, W.-J., R. Sharon, C. Xia, H. Kim, L.R. Johnson, P.G. Bruce, L.F. Nazar, Y.K. Sun, A.A. Frimer, M. Noked, S.A. Freunberger, and D. Aurbach, "Lithium-Oxygen Batteries and Related Systems: Potential, Status, and Future", *Chem. Rev*, vol. 120, pp. 6626-6683, 2020.

.2. Shao, Y., S. Park., J. Xiao, J.-G. Zhang, Y. Wang, and J. Liu, "Electrocatalysts for Nonaqueous Lithium-Air Batteries: Status, Challenges, and Perspective", *ACS Catal.,*. vol. 2, pp. 844-857, 2012.

3. Selvaraj, C., N. Munichandraiah, and L.G. Scanlon, "Dilithium Phthalocyanine as a catalyst for Oxygen Reduction in Non-Aqueous Li-O$_2$ Cells", *J. Porphyrin Phthalocyanines.,* vol. **16**, pp. 255-259, 2012.

4. Sun, D., Y. Shen, W. Zhang, L. Yu, Z. Yi, W. Yin, D. Wang, Y. Huang, J. Wang, D. Wang, and J.B. Goodenough, "A Solution-Phase Bifunctional Catalyst for Lithium-Oxygen Batteries", *J. Am. Chem. Soc.,* vol. **136**, pp. 8941-8946, 2014.

5. Mandal, S., R.N. Samajdar, S. Parida, S. Mishra, and A.J. Bhattacharyya "Transition Metal Phthalocyanines as Redox Mediators in Li-O2 Batteries: A Combined Experimental and Theoretical Study of the Influence of 3d Electrons in Redox Mediation", *ACS Appl. Mater. Interfaces,* vol. **14**, pp. 26714-26723, 2022.

6. Kichambare, P., S. Rodrigues, K. Hankins, P.B. Balbuena, W.A. Feld, and L. Scanlon, "Phthalocyanine as Catalyst for Rechargeable Lithium-Oxygen Batteries", *J. Porphyrin Phthalocyanines.,* vol. **26**, pp. 308-315, 2022.

7. Laoire, C.O., S. Mukerjee, K.M. Abraham, E.J. Plichta, and M.A. Hendrickson, "Influence of Nonaqueous Solvents on the Electrochemistry of Oxygen in the Rechargeable Lithium-Air Battery", *J. Phys..Chem. C.,* vol. **114**, pp. 9178-9186, 2010.

8. Bi, X., J. Li, M. Dahbi, J. Alami, K. Amine, and J. Lu, "Understanding the role of Lithium Iodide in Lithium-Oxygen Batteries", *Adv. Mater.,* vol. **34**, pp. 2106148, 2022.

9. Hu, L.-H., F.-Y. Wu, C.-T. Lin, A.N. Khlobystov, and L.-J. Li, "Graphene-modified LiFePO$_4$ cathode for lithium-ion battery beyond theoretical capacity", *Nature Comm.,* vol. **4**:1687, pp. 1-7, 2013.